


Asymmetric evolution of El Niño and La Niña: the recharge/discharge processes and role of the off-equatorial sea surface height anomaly

Zeng-Zhen Hu¹  · Arun Kumar¹ · Bohua Huang² · Jieshun Zhu^{1,3} · Rong-Hua Zhang⁴ · Fei-Fei Jin⁵

Received: 16 August 2016 / Accepted: 14 December 2016 / Published online: 20 December 2016
© Springer-Verlag Berlin Heidelberg (outside the USA) 2016

Abstract Observed oceanic and atmospheric anomalies in the tropical Pacific are analyzed to understand the symmetric and asymmetric characteristics between El Niño and La Niña evolutions. It is noted that the evolutions are largely symmetric for El Niño and La Niña prior to and in their mature phase, but become asymmetric afterwards. It is further demonstrated that this asymmetry is due to the fact that, on average, the discharge process associated with El Niño is stronger than the recharge counterpart associated with La Niña. The symmetric and asymmetric evolution for different phases of El Niño-Southern Oscillation (ENSO) is consistent with the associated recharge and discharge processes that are linked with the evolution of anomalous ocean surface current and gradient of sea surface height anomalies (SSHAs). It is suggested that the evolution of the meridional gradient of SSHAs in the central and eastern equatorial Pacific is different between El Niño and La Niña years due to relatively different rates of the SSHA changes on and off the equator. During the decay of a warm event, the equatorial SSHA quickly switches from positive

to negative, meanwhile the off-equator areas are occupied by positive SSHAs. Such changes on the equator and in the off-equatorial regions make the concavity of the meridional SSHA favorable for growth and persistence of westward surface zonal current anomaly in the equatorial Pacific, then for the ENSO phase transition. During the decay of a cold event, the slow decrease of the negative SSHA on the equator combined with the disappearance of the negative SSHA in the off-equatorial regions makes the meridional concavity reverse easily and is unfavorable for the steady growth of the eastward surface zonal current anomaly and for the phase transition. Thus, the asymmetric evolution of ENSO is associated with both the atmosphere and ocean anomalies on the equator and off the equator.

Keywords ENSO · Asymmetric evolution · Recharge and discharge processes · Meridional gradient of SSH

1 Introduction

Although the evolutions of the warm and cold phases of El Niño-Southern Oscillation (ENSO) are symmetric in many aspects (e.g., Philander 1990; An and Jin 2004; Sarachik and Cane 2010), they also display some prominent asymmetric features (Kumar and Hoerling 1997; Yu and Kim 2011; Anderson et al. 2013; Choi et al. 2013). For example, sea surface temperature (SST) anomalies (SSTAs) in the tropical Pacific associated with El Niño (warm) and La Niña (cold) years are asymmetric in terms of their meridional extent (Zhang et al. 2009), amplitude (Hoerling et al. 1997), and zonal phase propagation (McPhaden and Zhang 2009). On the other hand, the atmospheric responses associated with ENSO also demonstrate asymmetries (Hoerling et al. 1997), which

✉ Zeng-Zhen Hu
Zeng-Zhen.Hu@NOAA.GOV

¹ Climate Prediction Center, NCEP/NWS/NOAA, 5830
University Research Court, College Park, MD 20740, USA

² Department of Atmospheric, Oceanic, and Earth Sciences,
Center for Ocean-Land-Atmosphere Studies, George Mason
University, Fairfax, VA, USA

³ Earth System Science Interdisciplinary Center, University
of Maryland, College Park, MD 20740, USA

⁴ Key Laboratory of Ocean Circulation and Waves, Institute
of Oceanology, Chinese Academy of Sciences, Qingdao,
China

⁵ Department of Meteorology, University of Hawaii, 2525
Correa Road, HIG 350, Honolulu, HI 96822, USA

can partially be attributed to the asymmetry of the climatological state, upon which the warm and cold events evolve. As summarized in Hoerling et al. (1997), because of the zonal asymmetries of the climatology with SSTs being high in the west and low in the east, even small deviations of SST from its climatological condition can generate large rainfall anomalies in the western tropical Pacific, whereas warm SST anomalies with remarkable amplitudes are needed to induce convections over the cold tongue in the tropical eastern Pacific. Furthermore, negative SSTAs have no significant impact on the already climatologically dry conditions in the cold tongue region. The asymmetric response of the atmospheric convections associated with El Niño and La Niña may result in the

asymmetric response of the extra-tropical atmosphere to El Niño and La Niña.

One of the prominent features of the ENSO SST evolution is that the temporal evolution of El Niño and La Niña events is asymmetric. After their mature phase, for example, El Niño events generally decay by the next summer, but La Niña events often persist through the following year (Fig. 1c, d). Further, minor La Niña instead of an El Niño reemerges after major La Niña, clear departure from the concept of an ENSO cycle (Kessler 2002; Hu et al. 2014). Current ENSO theories, such as the recharge/discharge oscillator (e.g., Wyrtki 1985; Jin 1997a, b; Meinen and McPhaden 2000; Clarke et al. 2007), the delayed oscillator (e.g., Suarez and Schopf 1988; Battisti and Hirst 1989), as

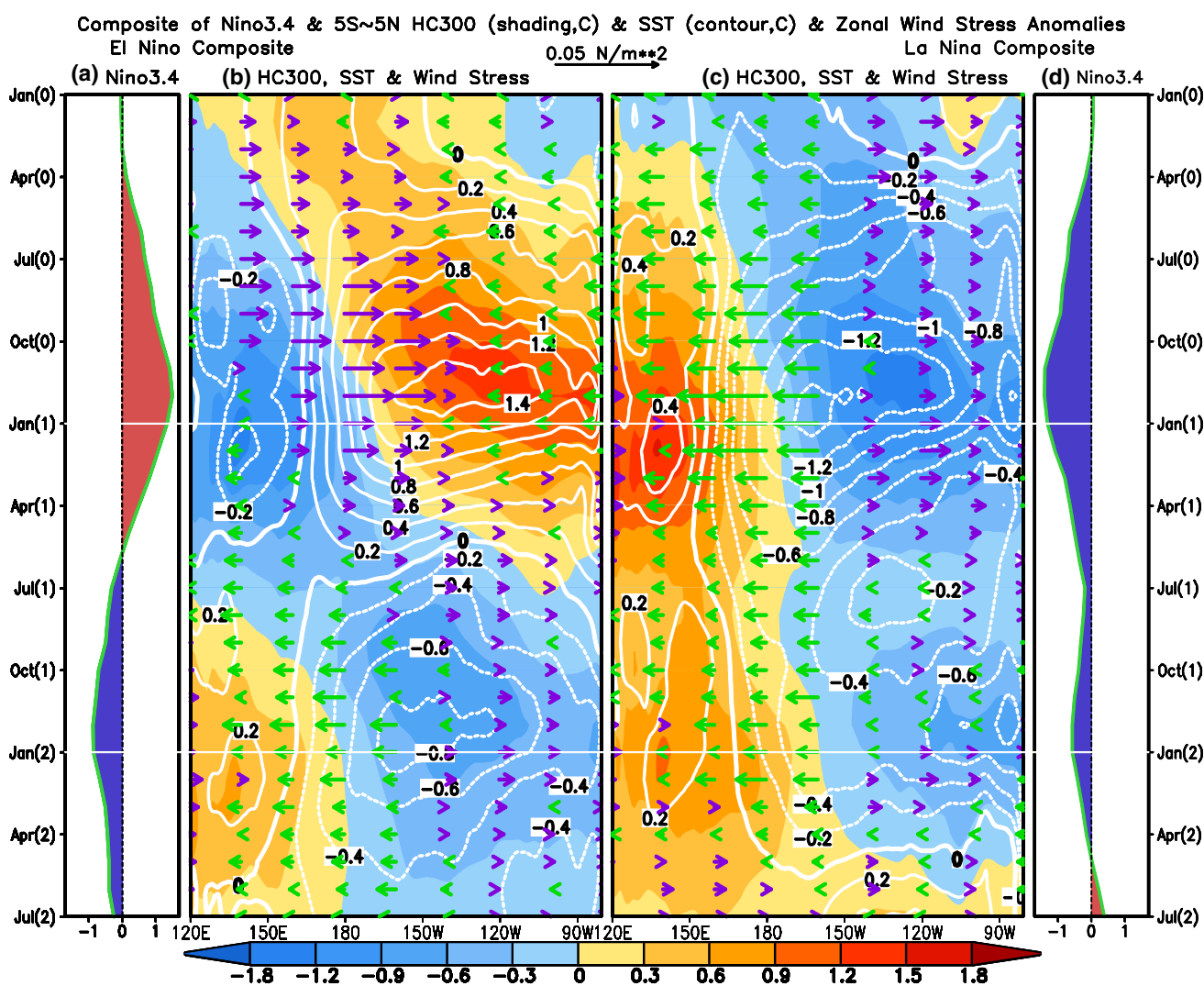


Fig. 1 Niño3.4 index composite for **a** El Niño and **d** La Niña years. Time and longitude evolutions of SST (contour), zonal component of surface wind stress (vector) and HC300 (shading) anomalies averaged between 5°S–5°N for composite of **b** El Niño and **c** La Niña years. The contour interval is 0.2 °C, and the unit is °C for HC300 and N/m²

for wind stress. The green (purple) vectors represent westward (eastward) wind stress anomalies. The white horizontal lines represent January of Year(1) and Year(2), respectively. The composites range from January of 1 year before the peak of ENSO [Year(0)] to July of second year after the peak [Year(2)]

well as others (e.g., Wang 2001), all imply a cyclic nature for ENSO whereby the climate over the tropical Pacific oscillates periodically between El Niño and La Niña states. The frequent occurrence of a second-year La Niña is a notable departure from the cyclic behavior.

The causes of temporal asymmetric evolution have been investigated. Some of the proposed causes include: (a) non-linearity of the atmospheric responses between the warm and cold events (e.g., Ohba and Ueda 2009); (b) the asymmetries in the meridional extent of the wind shift and its interaction with annual cycle (e.g. McGregor et al. 2013; Stuecker et al. 2013; Ren et al. 2016); (c) the asymmetric evolution in the oceanic response to wind forcing in delayed-oscillator conceptual model (e.g., Choi et al. 2013; DiNezio and Deser 2014); (d) asymmetry of reflected oceanic Rossby wave induced modification of ocean meridional gradient in association with meridional heat transport (Hu et al. 2014; Chen et al. 2016); and (e) contrast impact of remote oceans, such as the North Pacific (e.g., Alexander et al. 2010; Kim et al. 2012) and Indian (Kug et al. 2005; Okumura et al. 2011) Oceans.

Most of these previous works had demonstrated the importance of various nonlinearities in the asymmetry of the ENSO duration. The main difference between these studies is on the processes that produce the nonlinear behavior. For instance, Choi et al. (2013) emphasized the importance of the nonlinear relation between surface wind stress and SST anomalies. They noted that the wind stress anomalies depend more strongly on SSTAs during warm year than during cold year. DiNezio and Deser (2014) argued that different from El Niño, the thermocline doesn't show proportionally delayed response to La Niña intensity, and this nonlinearity determines the asymmetric duration of warm and cold events. These previous explanations are based on the nonlinear delayed oscillator framework of ENSO. However, there exists another framework for ENSO evolution—namely, the recharge/discharge oscillator and the question is whether the temporal asymmetry could be explained within this paradigm. According to the recharge/discharge theory (Jin 1997a, b), the discharge of equatorial heat content occurs during an El Niño, with a net heat transport from the equatorial to the off-equatorial regions. The reverse happens during a La Niña event, with heat being transported from the off-equatorial regions into the equatorial ocean. Within this framework, subsequent studies further elucidated the roles played by some specific equatorial physical processes, such as the zonal advection and the zonal wind-thermocline-SST feedback (e.g., An and Jin 2001; Zhang et al. 2007; Bejarano and Jin 2008; Ren and Jin 2013).

In this work, through composite analysis using observational and reanalysis data, the temporal evolution of oceanic and atmospheric anomalies in the equatorial Pacific

is examined to understand the symmetric and asymmetric features between El Niño and La Niña. The differences and similarities in the recharge and discharge processes in association with the warm and cold events are illustrated. Furthermore, surface ocean zonal and meridional geostrophic currents and their association with meridional gradient of SSH across the equator are examined. The remainder of this paper is organized as follows. Section 2 describes the data used in this work. The symmetric and asymmetric characteristics of El Niño and La Niña evolutions are displayed in Sect. 3. In particular, we examine the contrast of recharge and discharge processes connected with El Niño and La Niña and the role of the meridional gradient of SSHAs across the equator in the ENSO asymmetric evolution. Section 4 summarizes the results with some discussion.

2 Data

Monthly means of sea surface height (SSH), the 20 °C isotherm depth (D20), ocean heat content between the surface and the 300 m depth (HC300), and surface wind stress on a 1° × 1° grid are from the Global Ocean Data Assimilation System (GODAS) (Behringer and Xue 2004). In addition, we utilize monthly mean SST of the version 2 of the optimum interpolation (OIv2) on a 1° × 1° grid (Reynolds et al. 2002). All data used in this work cover the period January 1982–December 2015. Due to the fact that OIv2 does not have data before November, 1981, here the anomalies are referred to monthly climatologies in 1982–2011.

Two indices are used in the analysis. First one is the warm water volume (WWV) index which is defined as anomalous D20 depth averaged in (5°N–5°S, 120°E–80°W) (Meinen and McPhaden 2000). According to the recharge and discharge theory (see Eq. (4.2) of Jin 1997a), the WWV tendency is an indicator for the heat recharging and discharging strengths in the whole equatorial Pacific, which is negatively correlated with SSTA (Jin 1997a, b), and is associated with the phase turnaround of ENSO (Meinen and McPhaden 2000; Clarke et al. 2007; Kumar and Hu 2014). Another one is the Niño3.4 index which is defined as SSTA averaged in (5°S–5°N, 170°W–120°W) to measure the evolution of ENSO (Barnston et al. 1997). The ENSO year definition follows that of the NOAA Climate Prediction Center (CPC) based on 3-month running mean Niño3.4 index (see <http://www.cpc.ncep.noaa.gov/>). There are total 10 El Niño or 9 La Niña events during 1982–2015 (Table 1). Here, second year El Niño or La Niña is treated as a new event (see Table 1). Due to the fact that OIv2 SST starts from November 1981, we focus on ENSO events during 1982–2015. The composites start from January [January (0)] of the year of El Niño and La Niña development [Year(0)], and end by July [July(2)] of the year [Year(2)]

Table 1 El Niño and La Niña events selected in this work according to the definition of NOAA CPC based on 3-month running mean Niño3.4 index (see <http://www.cpc.ncep.noaa.gov/>)

El Niño events	La Niña events
1982–1983, 1986–1987, 1987–1988, 1991–1992, 1994–1995, 1997–1998, 2002–2003, 2004–2005, 2006–2007, 2009–2010	1984–1985, 1988–1989, 1995–1996, 1998–1999, 1999–2000, 2000–2001, 2007–2008, 2010–2011, 2011–2012

after their peak year. The Year(1) is referred to as the year of ENSO from mature to decay.

3 Symmetric and asymmetric evolution between El Niño and La Niña

3.1 SST, surface wind stress, and ocean heat content along the equator

From the Niño3.4 index composites (Fig. 1a, d), the asymmetric features between El Niño and La Niña evolutions are evident. The composite shows that, on average, both El Niño and La Niña years are followed by negative Niño3.4 index, indicating a non-cyclic nature of the ENSO evolution. To further compare the similarities and differences in the temporal evolutions of the warm and cold years, Fig. 1b, c show the corresponding composites of HC300, SST, and surface zonal wind stress anomalies on the equator (averaged between 5°S–5°N). For the HC300 anomaly composites (shading), it is noted that the anomaly starts to develop in the western Pacific in Year(0) in both the events, then propagates eastward. Later, through the Bjerknes air–sea interaction (Bjerknes 1969), the anomalies are further amplified, and peak around the winter of Year(0)–Year(1) in the central and eastern equatorial Pacific.

During the development phase, the anomalous patterns are quite symmetric between the warm and cold year composites. After their peaks, however, the asymmetric features are seen. For example, for the El Niño composite (Fig. 1b), in the early summer of Year(0), negative HC300 anomaly is observed in the western, while the positive anomaly in the central and eastern Pacific Ocean. For the negative HC300 anomalies to the west of the dateline, they are nearly stationary from the summer of Year(0) to the spring of Year(1). In the 2nd half of Year(1), they propagate eastward into the central Pacific, which is associated with the SST cooling in Year(1) as shown Fig. 1a. However, for the corresponding La Niña composite (Fig. 1c), throughout Year(0)–Year(1), the positive HC300 anomalies in the western equatorial ocean do not have corresponding eastward propagation. Instead, the negative anomalies of HC300 emerge locally in the central and eastern Pacific in the 2nd half of Year(1), suggesting that asymmetric

features between El Niño and La Niña become evident in the 2nd half of Year(1) and in Year(2).

The composite pattern of zonal surface wind stress anomalies (vectors in Fig. 1b, c) is physically consistent with the corresponding anomalous composites of SST and HC300. For example, anomalous westerly (easterly) wind stress is associated with reduction (enhancement) of anomalous zonal gradients of SST and HC300 (Bjerknes 1969; Wyrtki 1985; Philander 1990; Sarachik and Cane 2010). Corresponding to the evolutions in SSTAs, westerly anomalies switch to easterly anomalies over the western and central equatorial ocean in late winter and spring for the El Niño composite, while the easterly anomalies persist for 2 years with no sign changes for the La Niña composite, consistent with the findings of Ohba and Ueda (2009).

Overall, the composite evolution analyses suggest that the anomalies on the equator are basically symmetric in the El Niño and La Niña composites prior to and in their mature phase. The temporal evolution becomes asymmetric after the mature phase. Since the recharge and discharge of water mass on and off the equator play a critical role in the ENSO evolutions and its phase turnaround, the asymmetry in the evolutions between El Niño and La Niña can be associated with differences in the recharge and discharge processes, which are addressed below.

3.2 Symmetry and asymmetry of recharge and discharge processes

The symmetric and asymmetric characteristics between the El Niño and La Niña composites are also reflected in the recharge–discharge process. The ocean heat accumulation or disappearance is an indicator for the ENSO phase turnaround (Jin 1997a, b). In essence, the recharge–discharge theory argues that the convergence (divergence) of meridional geostrophic current recharges (discharges) the WWV in the equatorial Pacific during La Niña (El Niño), leading to a zonally integrated deepening (shoaling) of equatorial thermocline, meaning recharging (discharging) mass and heat into (from) the upper equatorial Pacific. After the equatorial Pacific is recharged (or discharged), some feedbacks (such as the thermocline feedback and the zonal advective feedback) tend to work constructively (Suarez and Schopf 1988; Battisti and Hirst 1989; Picaut

et al. 1997; Jin and An 1999; Ren and Jin 2013), leading to a phase transition of ENSO.

Here, the tendency of the WWV index is used to represent the recharge and discharge processes. The composites show that the overall WWV tendency (shading in Fig. 2a, b) is out of phase with Niño3.4 index (solid curve in Fig. 2a, b), consistent with the recharge and discharge theory (Jin 1997a, b): El Niño (La Niña) is overall associated with the negative (positive) WWV tendency due to discharge (recharge) processes, although there are outliers (negative (positive) WWV tendency in some months of La Niña (El Niño) years, see Fig. 3a). Despite the overall synchronization between the WWV tendency and Niño3.4 index, some differences are noted for the relationship between the El Niño and La Niña composites (Fig. 2c). For example, the overall discharge intensity during El

Niño [October(0)–April(1)] is stronger than its recharge counterpart during La Niña (Figs. 2, 3). As a result, the sum of El Niño and La Niña composites (Fig. 2c), which reflects the asymmetric evolution, is mainly discharge during November (0)–October(1) and recharge during November(1)–June(2). The latter probably reflects the fact that the La Niña events linger longer. Specifically, the maximum discharge for individual El Niño event reaches about -8 m per month for WWV tendency, while the maximum recharge for individual La Niña event is only about 5 m per month for WWV tendency (Fig. 3a).

Interestingly, the connection of the recharge and discharge processes with Niño3.4 SSTA, which can be approximated by linear regression coefficient of WWV tendency onto Niño3.4 SSTA, seems to also have some differences (Fig. 3a). Specifically, the regression coefficient of WWV

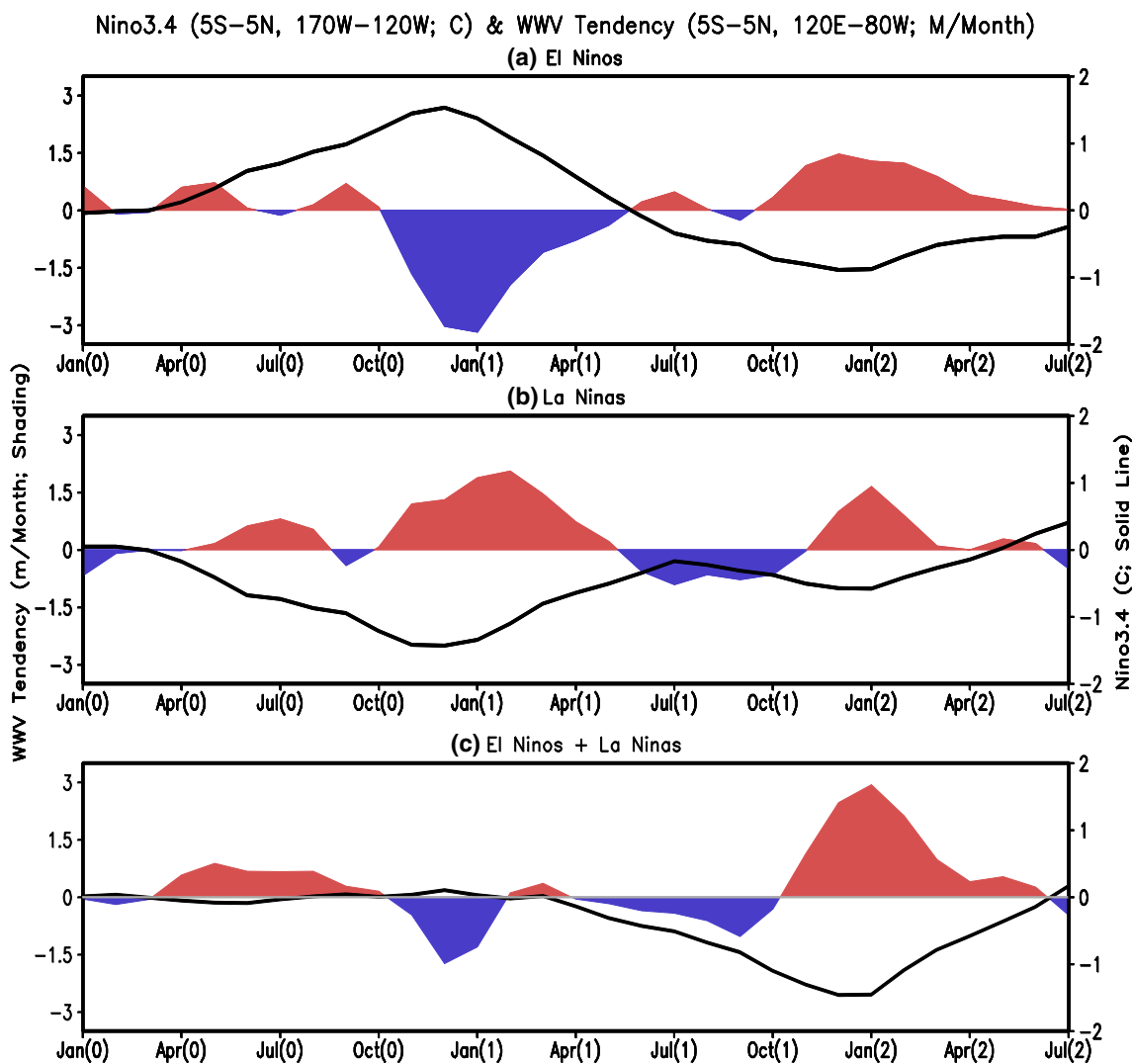


Fig. 2 Time evolutions of the WWV index anomalous tendency (shading), and Niño3.4 index (solid curve) for composite of a El Niño and b La Niña years, and c El Niño + La Niña years ((a)+(b)).

The WWV index is defined as the D20 anomaly averaged in (5°S–5°N, 120°E–80°W). The unit is m/month for the WWV anomalous tendency and °C for Niño3.4 index

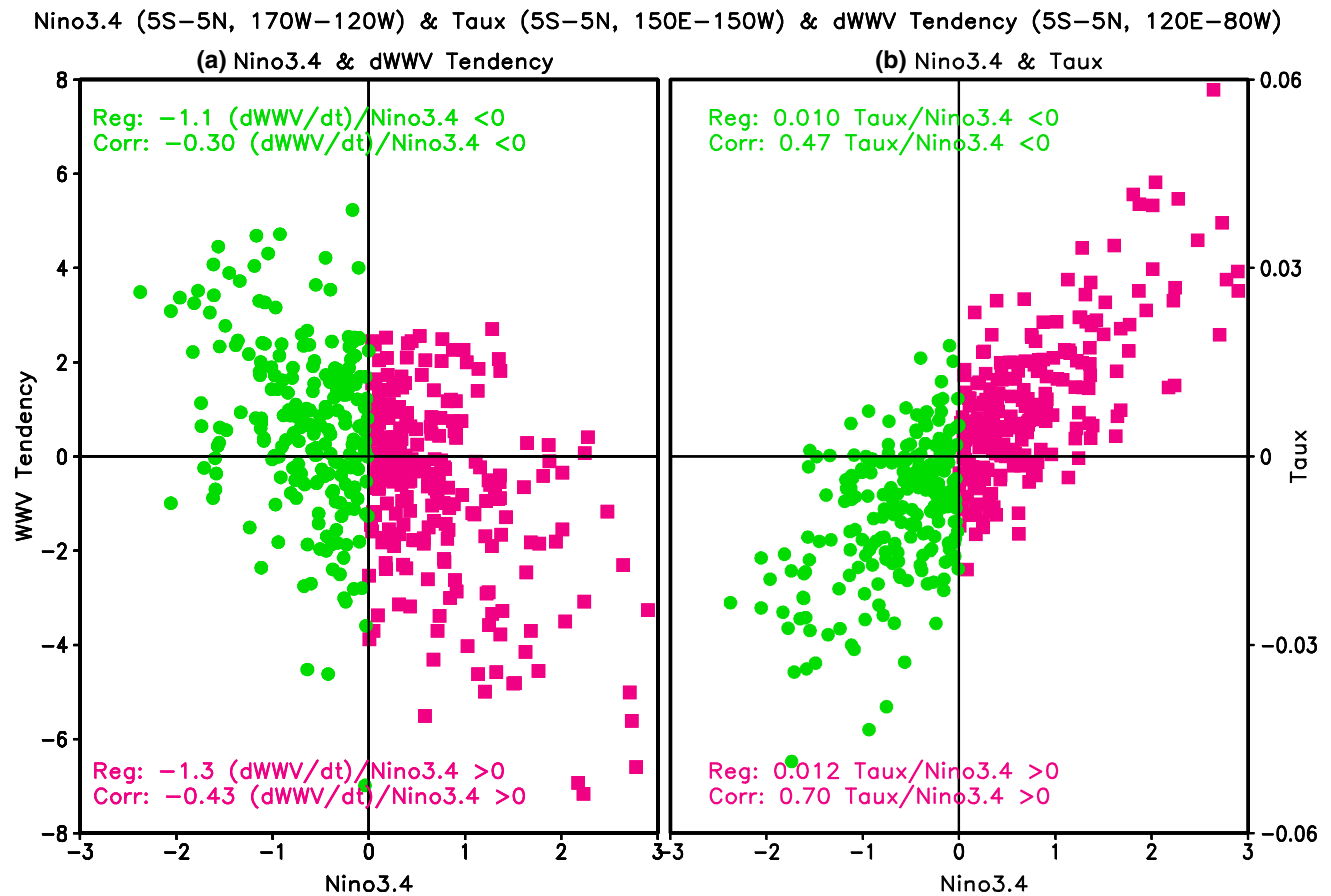


Fig. 3 Scatter plots of monthly mean anomalies of **a** Niño3.4 index (x-axis) and WWV tendency index (y-axis) and **b** Niño3.4 index (x-axis) and zonal wind stress (Taux) averaged in (5°S–5°N, 150°E–150°W) (y-axis) for positive Niño3.4 index (red squares) and negative Niño3.4 index (green squares). The regression coefficient of WWV anomalous tendency (zonal wind stress) onto Niño3.4 index

is -1.3 m/(month °C) (0.012 N/m²) for positive Niño3.4 index and -1.1 m/(month °C) (0.010 N/m²) for negative Niño3.4 index. The correlation is -0.43 (-0.30) between Niño3.4 index and WWV tendency index, and 0.70 (0.47) between Niño3.4 index and zonal wind stress for positive (negative) Niño3.4 index

tendency onto Niño3.4 SSTA is -1.3 m/(month °C) for the positive Niño3.4 months and it is -1.1 m/(month °C) for the negative Niño3.4 months (Fig. 3a). Consistently, the correlation between WWV tendency and Niño3.4 SSTA is higher for positive Niño3.4 months (-0.43) than for negative Niño3.4 months (-0.30) (Fig. 3a).

Furthermore, the relationship between Niño3.4 index and zonal wind stress averaged in (5°S–5°N, 150°E–150°W; it is so-called Niño4 region) also has some differences between positive and negative Niño3.4 index (Fig. 3b). For instance, the regression coefficient of zonal wind stress onto Niño3.4 index is 0.012 N/(m² °C) for positive Niño3.4 index and 0.010 N/(m² °C) for negative Niño3.4 index. Their corresponding correlation is 0.70 (0.47) for positive (negative) Niño3.4 index (Fig. 3b). The relationship between Niño3.4 SSTA and zonal wind stress in Niño4 region mainly reflects the intensity of the so-called Bjerknes feedback (Bjerknes 1969; Lloyd et al. 2009). The connections among Niño4 SST, WWV and

zonal wind stress anomalies shown in Fig. 3 are the feature of air-sea coupling in the equatorial Pacific.

While, the amplitude differences of the numbers shown in Fig. 3a, b suggest that statistically zonal wind stress anomaly is more closely connected with Niño3.4 than WWV tendency does. On the other hand, the different regression and correlation coefficient values between positive and negative Niño3.4 index (Fig. 3) suggest that on average, air-coupling is stronger in El Niño years than in La Niña years. That is generally consistent with some previous works. For example, both McGregor et al. (2013) and DiNezio and Deser (2014) noted that the discharge of oceanic heat content increase as an El Niño becomes intensified in its amplitude, but the recharge is insensitive to the amplitude of La Niña. However, if from the view of the linear regression and correlation, the differences seem not as significant as these previous works indicated. Overall, these results suggest that, consistent with the fact that, on average, the SSTA amplitude in El Niño is larger than that

in La Niña, and the anomalous discharge during El Niño is stronger than the anomalous recharge during La Niña. Also, the linear relationship between discharge/recharge and Niño3.4 SSTA has some differences between warm and cold events.

3.3 Connection with zonal and meridional currents and role of off-equatorial SSHA

According to Jin and An (1999), recharge/discharge process is associated with the meridional (V_g) convergence and zonal gradient of thermocline depth on the equator that is tied up with the meridional concavity of the thermocline anomalies and zonal (U_g) component of the geostrophic current anomalies of upper ocean. Here, geostrophic current (U_g and V_g) is computed at latitudes of 4.5°S, 3.5°S, 2.5°S, 1.5°S, 0.5°S, 0.5°N, 1.5°N, 2.5°N, 3.5°N, and 4.5°N, then do the average to get the mean between 5°S and 5°N. For the calculation of the meridional geostrophic current, SSHA averaged in 156°E–140°W is used. According to Clarke et al. (2007; see their Figs. 3 and 7), the ocean heat recharge/discharge process takes place mainly in the western and central equatorial Pacific (156°E–140°W). In the other words, the SSHA in this longitude zonal is largely associated with ocean heat exchange between the equator and the off-equator, while the SSTA in the region east of 140°E may be due to the zonal propagation of the ocean heat along the equator.

The composites shown in Figs. 4, 5, and 6 are consistent with the schematic evolution of Jin and An (1999; see their Fig. 2). Specifically, both pronounced anomalous eastward zonal current and anomalous divergence of meridional current on the equator and positive SSHA in the central and eastern tropical Pacific are present during the El Niño phase (Figs. 4a, 5a, 6a; July(0)–January(1)). Meanwhile, both notable anomalous westward zonal current and anomalous convergence of meridional current on the equator and negative SSHA in the central and eastern tropical Pacific are present during the La Niña phase (Figs. 4b, 5b, 6b; July(0)–January(1)). During the transition phase [both from the warm to the cold phase and from the cold to the warm phase during April (1)–July(1)], the zonal current and SSHAs reverse their sign, and anomalous meridional current on the equator becomes smaller.

The equatorial surface zonal current reversal in January(1) originates from the reversal of meridional gradient of SSHA. In general, the zonally averaged SSHA and the meridional gradient are largely symmetric with respect to the equator before July(1). Using El Niño composite as an example (Figs. 4a, 5a), SSHA has its maximum on the equator during Year(0). After January(1), because the equatorial SSHA becomes the minimum in meridional direction due to the decrease of SSHA on the equator and

the increase of SSHAs on both sides of the equator. The decrease on the equator and increase in the off-equatorial region in SSHA may be associated with the discharge due to poleward heat transports along the equator and the reflected equatorial Rossby waves along the off-equator at the eastern boundary (Hu et al. 2014). These changes reverse the concavity of the SSHA meridional profile and thus lead to the reversal in surface zonal current through geostrophic balance (Jin and An 1999; Chen et al. 2016). Therefore, the establishment of the off-equatorial SSHAs and the weakening of the equatorial SSHA may be a cause of the surface zonal current reversal and its subsequent sustenance from January(1) to July(1) (Figs. 4a, 5a). The La Niña event (Figs. 4b, 5b) is largely a mirror image of the El Niño process described above and the two are symmetric in their evolution before July(1).

After July(1), when the off-equatorial SSHAs move outside the equatorial wave-guide, the asymmetry of the evolutions between El Niño and La Niña emerges. In particular, the direction of the surface zonal current reverses again in the cold event but sustained in the warm one (Fig. 4). The differences in surface zonal current evolutions of the warm and cold events can be explained by the changes in the meridional gradient of SSHA and the different rates of the SSHA changes between the equatorial and the off-equatorial Pacific. For the warm event (Figs. 4a, 5a), the equatorial SSHA quickly switches from positive to negative around January(1)–April(1), meanwhile the off-equator is occupied by positive SSHAs in the north and by relatively smaller negative SSHAs in the south. Such changes on the equator and in the off-equator after January(1) make the concavity of the meridional SSHA profile favorable for growth and continuation of westward surface zonal current anomaly in the equatorial Pacific. For the cold event (Figs. 4b, 5b), the decay of the cold equatorial anomaly from January(1) to July(1) is much slower and the warm anomalies do not get well established by July(1). The overall weak recharge process seems associated with the slower demise of the cold SSTA during La Niña. After the off-equatorial negative SSHA disappears, the concavity is easily reversed and the westward surface zonal current anomaly, once again, starts to enhance the cold signals on the equator. Therefore, the relatively different rates of the equatorial and off-equatorial SSHA changes from January(1) to July(1) are a key feature of the ENSO asymmetry during Year(1).

The evolutions of the zonal and meridional current as well as the SSH anomalous composites (Figs. 4, 5) are consistent with the symmetric and asymmetric features of discharge/recharge processes associated with the ENSO evolution. These anomalies are symmetric for El Niño and La Niña prior to and in their mature phase, and become asymmetric afterwards. Post the peak phases of ENSO

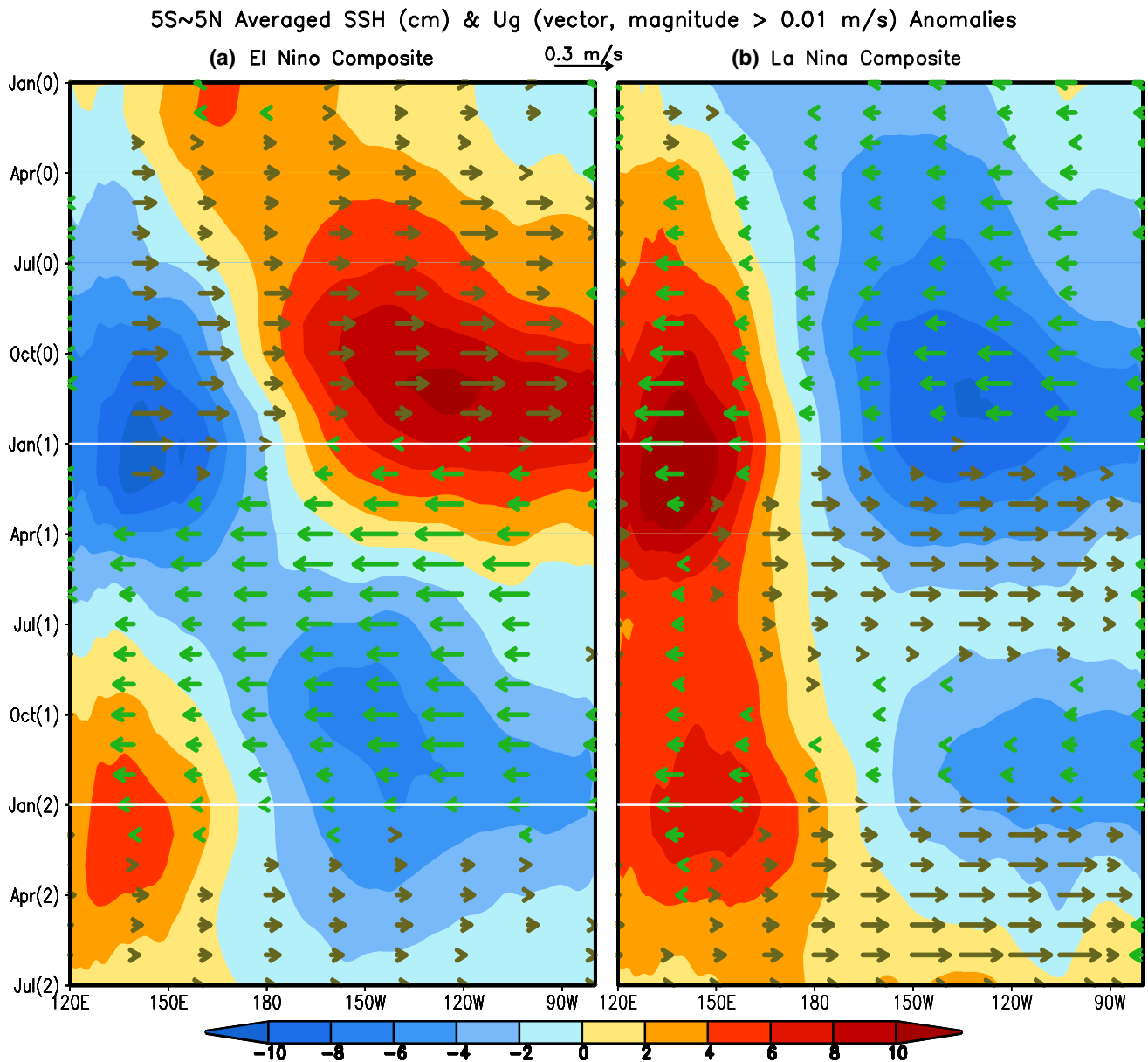


Fig. 4 Time and longitude evolutions of zonal geostrophic current anomaly at the ocean surface (*vector*) and SSHA (*shading*) averaged in 5°S–5°N for composites of **a** El Niño and **b** La Niña years. The

green (golden) vectors are for westward (eastward) current. The *white lines* represent January(1) and January(2), respectively

[January(1)–January(2)], anomalous westward zonal current and anomalous convergence of meridional current are pronounced and persistent for the El Niño composite (Figs. 4a, 5a, 6a), while for the La Niña composite, the notable anomalous eastward zonal current is disrupted by weak westward anomaly during August(1)–December(1) (Fig. 4b) and the anomalous convergence of meridional current persists (Figs. 5b, 6b). The lack of persistence of an anomalous eastward current and thus the lack of eastward advection of warm ocean temperature prevent the eastward surge of the warm water. This is consistent with the

fact that instead of evolving to an El Niño, a La Niña often has “double-dip”, meaning persistent into second year or reemergence of a second year La Niña (e.g., Kessler 2002; Hu et al. 2014).

4 Summary and discussion

In this work, the evolutions of oceanic and atmospheric anomalies in the tropical Pacific are analyzed to show the symmetric and asymmetric features between El Niño and

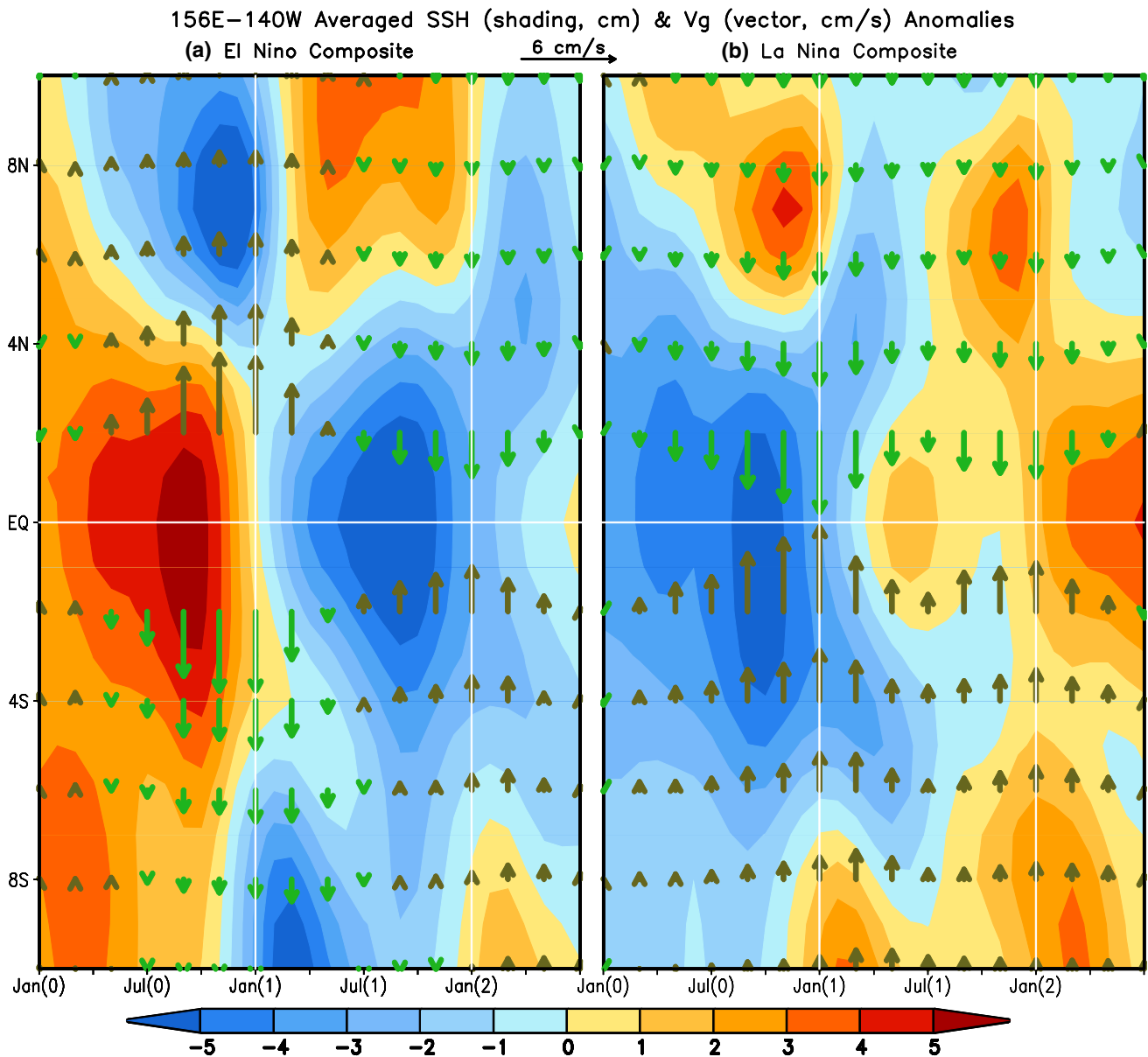


Fig. 5 Time and latitude evolutions of meridional geostrophic current anomaly at the ocean surface (*vector*) and SSHA (*shading*) averaged in 156°E–140°W for composites of **a** El Niño and **b** La Niña

years. The *green* (*golden*) vectors are for southward (northward) current. The *white lines* represent the equator, January(1), and January(2), respectively

La Niña through composite analysis using observation-based reanalysis data. The differences and similarities in the recharge and discharge processes associated with El Niño and La Niña evolution are examined, and the possible influence of the off-equatorial sea surface height is investigated.

It is noted that the evolutions of ocean and atmospheric anomalies along the equator in the El Niño and La Niña composites are symmetric before and during their mature phase. However, the evolutions become asymmetric afterwards. It is also noted that, on average, the

discharge intensity during El Niño is stronger than its recharge counterpart associated with La Niña. The symmetric and asymmetric evolution for different phases of El Niño–Southern Oscillation (ENSO) is consistent with the associated recharge and discharge processes that are linked with the evolution of anomalous ocean surface current and gradient of sea surface height anomalies (SSHAs). It is suggested that the evolution of the meridional gradient of SSHAs in the equatorial Pacific is different between El Niño and La Niña years due to different rates of the relative SSHA changes on and off the equator.

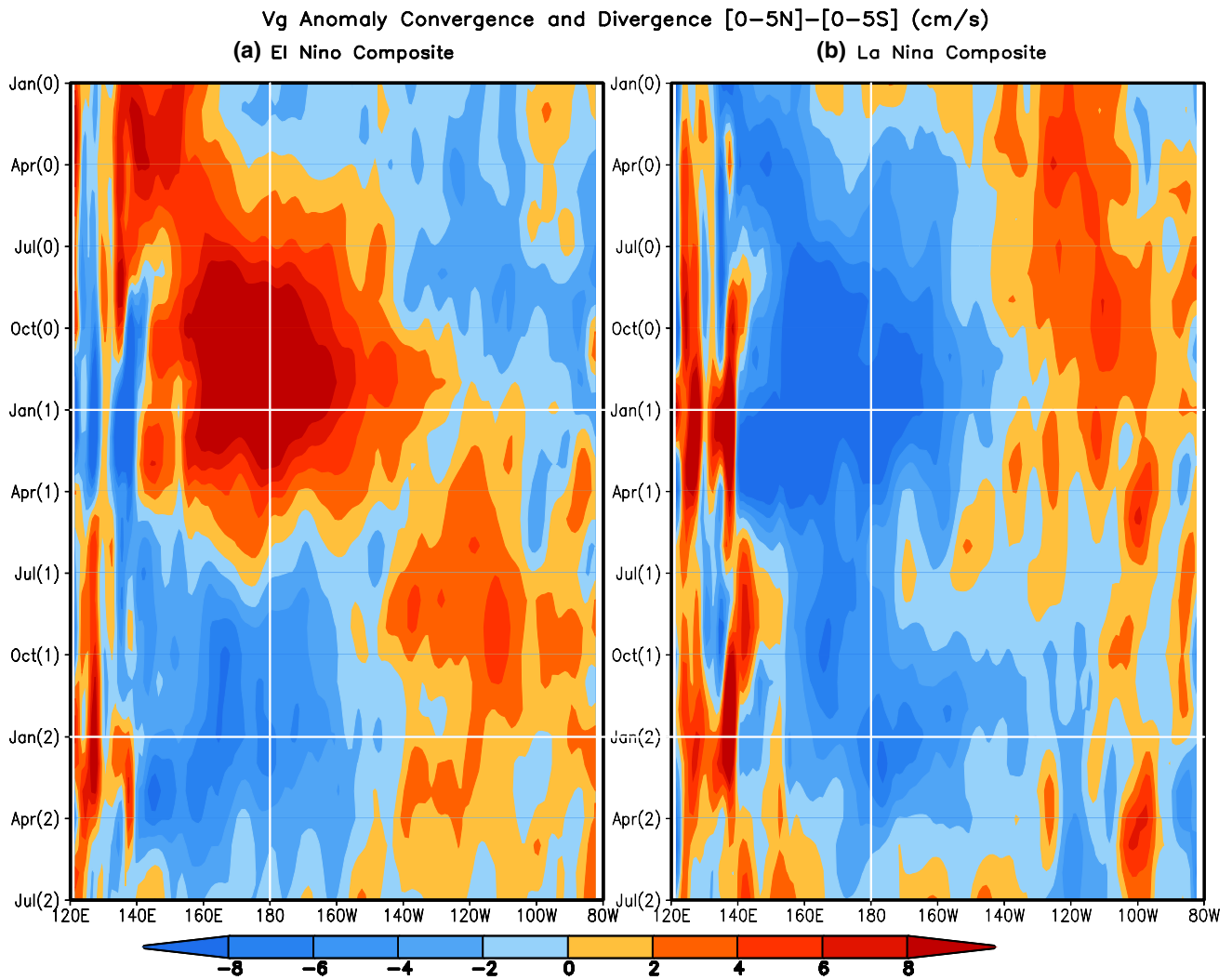


Fig. 6 Same as Fig. 4, but for divergence and convergence of meridional geostrophic current anomaly at the ocean surface, which is defined as the difference of mean in 0° – 5° N minus mean in 5° S– 0°

During the decaying phase of a warm event, the equatorial SSHA quickly switches from positive to negative, meanwhile the off-equatorial regions are occupied by positive SSHAs. Such changes on the equator and in the off-equator make the concavity of the meridional SSHA profile favorable for the westward surface zonal current anomaly in the equatorial Pacific and for the ENSO phase transition. During the decaying phase of a cold event, the slow decrease of the negative SSHA on the equator combined with the disappearance of the negative SSHA in the off-equator make the meridional concavity easily reverse and is unfavorable for the steady growth of the eastward surface zonal current and for the phase transition. The persistently weaker recharge process seems to be the major reason for the slower demise of the cold SSTA during La Niña and its revival around July(1). Thus, the asymmetric evolution of ENSO is associated with both

the atmosphere and ocean anomalies on the equator and also in the off-equatorial regions.

What causes the asymmetry between recharge and discharge processes associated with ENSO after their peak phases? We speculate that the answer may lie in the specific water properties transported from the off-equatorial to the equatorial ocean. For example, Fig. 5b shows that, from April(1) to July(1) after La Niña peak, the convergence of V_g brings negative SSHA from the off-equatorial oceans of both hemispheres into the equatorial ocean, which may cause the termination of the recharge process and cool the equator. That terminates the transition from La Niña to El Niño and leads to asymmetric evolution between El Niño and La Niña. Hu et al. (2014) argued that the cold ocean temperature anomaly or the negative SSHA over the off-equatorial region may be associated with the Rossby wave signal reflected at the American coast of the Pacific.

Our current work proposes the possible role of the meridional gradient of thermocline and the off-equatorial SSHA resulting in the asymmetric evolution of recharge and discharge of ocean and ENSO. In fact, the asymmetric evolution of ENSO may also be partially due to other nonlinear interactions. Jin et al. (2003), Stuecker et al. (2013), and Ren et al. (2016) argued that the interaction between the ENSO time scale variation and climatological annual cycle can generate near-annual time scale variation, which may turn out to affect the recharge and discharge processes associated with ENSO and then the evolution of ENSO. Furthermore, as discussed in the Sect. 1, the crucial role of climatological state of the tropical Pacific atmosphere played in the asymmetric evolution of ENSO had been proposed (Hoerling et al. 1997; Ohba and Ueda 2009).

Last, in this work, WWV tendency is used as a proxy to measure the charge/discharge processes. WWV includes all processes that alter heat content, which are dominated by changes in thermocline depth on interannual timescales. Hence the WWV can be seen as a surrogate for thermocline depth. This relationship might not necessarily work on seasonal timescales, because horizontal advection is more dominant. In addition, the results in this work are based on composite of ENSO events since 1982 and largely rely on products of one ocean data assimilation system (GODAS). The impact of biases in GODAS, particularly artificial ocean internal sources and sinks of heat introduced during assimilation process (Huang et al. 2010; Hu et al. 2016) should be identified and estimated through comparison by analyzing multiple oceanic reanalyzed datasets. Furthermore, it should be pointed out that the robustness and possible interdecadal dependence of the results should be verified by using independent and longer observational or modeling data (Zhang et al. 1999; Hu et al. 2017).

Acknowledgements Authors appreciate the constructive comments of two reviewers as well as Dr. Peitao Peng and Prof. Raghu Murtugudde. Zhang is supported by the IOCAS through the CAS Strategic Priority Project [the Western Pacific Ocean System (WPOS)] and the NSFC-Shandong Joint Fund for Marine Science Research Center (Grant No. U1406401). Huang is supported by grants from NSF (ATM-0830068), NOAA (NA09OAR4310058), and NASA (NNX-09AN50G). All data for this paper are available at NOAA Climate Prediction Center (CPC) and National Climate Data Center (NCDC), (<http://www.cpc.ncep.noaa.gov/products/GODAS/>; <http://nomads.ncdc.noaa.gov/data.php?name=access#cfs>). The scientific results and conclusions, as well as any view or opinions expressed herein, are those of the authors and do not necessarily reflect the views of NWS, NOAA, or the Department of Commerce.

References

Alexander MA, Vimont DJ, Chang P, Scott JD (2010) The Impact of extratropical atmospheric variability on ENSO: testing the

- seasonal footprinting mechanism using coupled model experiments. *J Clim* 23:2885–2901. doi:[10.1175/2010JCLI3205.1](https://doi.org/10.1175/2010JCLI3205.1)
- An S-I, Jin F-F (2001) Collective role of zonal advective and thermocline feedbacks in ENSO mode. *J Clim* 14:3421–3432
- An S-I, Jin F-F (2004) Nonlinearity and asymmetry of ENSO. *J Clim* 17:2399–2412
- Anderson BT, Furtado JC, Cobb KM, Di Lorenzo E (2013) Extratropical forcing of El Niño/Southern Oscillation asymmetry. *Geophys Res Lett* 40:4916–4921. doi:[10.1002/grl.50951](https://doi.org/10.1002/grl.50951)
- Barnston AG, Chelliah M, Goldenberg SB (1997) Documentation of a highly ENSO-related SST region in the equatorial Pacific. *Atmos Ocean* 35:367–383
- Battisti DS, Hirst AC (1989) Interannual variability in a tropical atmosphere–ocean model: Influence of the basic state, ocean geometry and nonlinearity. *J Atmos Sci* 46:1687–1712
- Behringer DW, Xue Y (2004) Evaluation of the global ocean data assimilation system at NCEP: the Pacific Ocean. preprints, eighth symposium on integrated observing and assimilation systems for atmosphere, oceans, and land surface, American Meteor Society, Seattle
- Bejarano L, Jin F-F (2008) Coexistence of equatorial coupled modes of ENSO. *J Clim* 21:3051–3067. doi:[10.1175/2007JCLI1679.1](https://doi.org/10.1175/2007JCLI1679.1)
- Bjerknes J (1969) Atmospheric teleconnections from the equatorial Pacific. *Mon Weather Rev* 97:163–172
- Chen H-C, Hu Z-Z, Huang B, Sui C-H (2016) The role of reversed equatorial zonal transport in terminating an ENSO event. *J Clim* 29(16):5859–5877. doi:[10.1175/JCLI-D-16-0047.1](https://doi.org/10.1175/JCLI-D-16-0047.1)
- Choi K, Vecchi G, Wittenberg A (2013) ENSO transition, duration and amplitude asymmetries: Role of the nonlinear wind stress coupling in a conceptual model. *J Clim* 26:9462–9476. doi:[10.1175/JCLI-D-13-00045.1](https://doi.org/10.1175/JCLI-D-13-00045.1)
- Clarke AJ, Van Gorder S, Colantuono G (2007) Wind stress curl and ENSO discharge/recharge in the equatorial Pacific. *J Phys Ocean* 37(4):1077–1091
- DiNezio P, Deser C (2014) Nonlinear controls on the persistence of La Niña. *J Clim* 27(19):7335–7355. doi:[10.1175/JCLI-D-14-00033.1](https://doi.org/10.1175/JCLI-D-14-00033.1)
- Hoerling M, Kumar A, Zhong M (1997) El Niño, La Niña, and the nonlinearity of their teleconnections. *J Clim* 10:1769–1786
- Hu Z-Z, Kumar A, Xue Y, Jha B (2014) Why were some La Niñas followed by another La Niña? *Clim Dyn* 42(3–4):1029–1042. doi:[10.1007/s00382-013-1917-3](https://doi.org/10.1007/s00382-013-1917-3)
- Hu Z-Z, Kumar A, Huang B (2016) Spatial distribution and the interdecadal change of leading modes of heat budget of the mixed-layer in the tropical Pacific and the association with ENSO. *Clim Dyn* 46(5–6):1753–1768. doi:[10.1007/s00382-015-2672-4](https://doi.org/10.1007/s00382-015-2672-4)
- Hu Z-Z, Kumar A, Huang B, Zhu J, Ren H-L (2017) Interdecadal variations of ENSO around 1999/2000. *J Meteor Res* (published online). doi:[10.1007/s13351-017-6074-x](https://doi.org/10.1007/s13351-017-6074-x)
- Huang B, Xue Y, Zhang D, Kumar A, McPhaden MJ (2010) The NCEP GODAS ocean analysis of the tropical Pacific mixed layer heat budget on seasonal to interannual time scales. *J Clim* 23:4901–4925
- Jin F-F (1997a) An equatorial ocean recharge paradigm for ENSO. Part I: conceptual model. *J Atmos Sci* 54:811–829
- Jin F-F (1997b) An equatorial ocean recharge paradigm for ENSO. Part II: a stripped-down coupled model. *J Atmos Sci* 54:830–847
- Jin F-F, An S-I (1999) Thermocline and zonal advective feedbacks within the equatorial ocean recharge oscillator model for ENSO. *J Geophys Res* 26:2989–2992
- Jin F-F, Kug J, An S-I (2003) A near-annual coupled mode in the equatorial Pacific Ocean. *Geophys Res Lett* 30:1080. doi:[10.1029/2002GL015983](https://doi.org/10.1029/2002GL015983)
- Kessler WS (2002) Is ENSO a cycle or a series of events? *Geophys Res Lett* 29(23):2125. doi:[10.1029/2002GL015924](https://doi.org/10.1029/2002GL015924)

- Kim ST, Yu J-Y, Kumar A, Wang H (2012) Examination of the two types of ENSO in the NCEP CFS model and its extratropical associations. *Mon Weather Rev* 140:1908–1923. doi:[10.1175/MWR-D-11-00300.1](https://doi.org/10.1175/MWR-D-11-00300.1)
- Kug J-S, An S-I, Jin F-F, Kang I-S (2005) Preconditions for El Niño and La Niña onsets and their relation to the Indian Ocean. *Geophys Res Lett* 32:L05706. doi:[10.1029/2004GL021674](https://doi.org/10.1029/2004GL021674)
- Kumar A, Hoerling MP (1997) Interpretation and implications of observed inter-El Niño variability. *J Clim* 10:83–91
- Kumar A, Hu Z-Z (2014) Interannual variability of ocean temperature along the equatorial Pacific in conjunction with ENSO. *Clim Dyn* 42(5–6):1243–1258. doi:[10.1007/s00382-013-1721-0](https://doi.org/10.1007/s00382-013-1721-0)
- Lloyd J, Guilyardi E, Weller H, Slingo J (2009) The role of atmosphere feedbacks during ENSO in the CMIP3 models. *Atmos Sci Lett* 10:170–176
- McGregor S, Ramesh N, Spence P, England MH, McPhaden MJ, Santoso A (2013) Meridional movement of wind anomalies during ENSO events and their role in event termination. *Geophys Res Lett* 40:749–754. doi:[10.1002/grl.50136](https://doi.org/10.1002/grl.50136)
- McPhaden MJ, Zhang X (2009) Asymmetry in zonal phase propagation of ENSO sea surface temperature anomalies. *Geophys Res Lett* 36:L13703. doi:[10.1029/2009GL038774](https://doi.org/10.1029/2009GL038774)
- Meinen CS, McPhaden MJ (2000) Observations of warm water volume changes in the equatorial Pacific and their relationship to El Niño and La Niña. *J Clim* 13:3551–3559
- Ohba M, Ueda H (2009) Role of nonlinear atmospheric response to SST on the asymmetric transition process of ENSO. *J Clim* 22:177–192
- Okumura YM, Ohba M, Deser C, Ueda H (2011) A proposed mechanism for the asymmetric duration of El Niño and La Niña. *J Clim* 24:3822–3829. doi:[10.1175/2011JCLI3999.1](https://doi.org/10.1175/2011JCLI3999.1)
- Philander SGH (1990) *El Niño, La Niña and the Southern Oscillation*. Academic Press, San Diego, p 293 (ISBN 0125532350)
- Picaut J, Masia F, du Penhoat Y (1997) An advective-reflective conceptual model for the oscillatory nature of ENSO. *Science* 277:663–666
- Ren H, Jin F-F (2013) Recharge oscillator mechanisms in two types of ENSO. *J Clim* 26:6506–6523. doi:[10.1175/JCLI-D-12-00601.1](https://doi.org/10.1175/JCLI-D-12-00601.1)
- Ren H-L, Zuo J, Jin F-F, Stuecker MF (2016) ENSO and annual cycle interaction: the combination mode representation in CMIP5 models. *Clim Dyn* 46:3753–3765. doi:[10.1007/s00382-015-2802-z](https://doi.org/10.1007/s00382-015-2802-z)
- Reynolds RW, Rayner NA, Smith TM, Stokes DC, Wang W (2002) An improved in situ and satellite SST analysis for climate. *J Clim* 15:1609–1625
- Sarachik ES, Cane MA (2010) *The El Niño-Southern Oscillation Phenomenon*. Cambridge University Press, London, p 384
- Stuecker MF, Timmermann A, Jin F-F, McGregor S, Ren H-L (2013) A combination mode of the annual cycle and the El Niño/Southern Oscillation. *Nat Geosci* 6:540–544. doi:[10.1038/ngeo1826](https://doi.org/10.1038/ngeo1826)
- Suarez MJ, Schopf PS (1988) A delayed action oscillator for ENSO. *J Atmos Sci* 45:3283–3287
- Wang C (2001) A unified oscillator model for the El Niño-Southern Oscillation. *J Clim* 14:98–115
- Wyrtki K (1985) Water displacements in the Pacific and the genesis of El Niño cycles. *J Geophys Res* 90(C4):7129–7132
- Yu J-Y, Kim ST (2011) Reversed spatial asymmetries between El Niño and La Niña and their linkage to decadal ENSO modulation in CMIP3 models. *J Clim* 24:5423–5434. doi:[10.1175/JCLI-D-11-00024.1](https://doi.org/10.1175/JCLI-D-11-00024.1)
- Zhang R-H, Rothstein LM, Busalacchi AJ (1999) Interannual and decadal variability of the subsurface thermal structure in the Pacific Ocean: 1961–1990. *Clim Dyn* 15:703–717
- Zhang Q, Kumar A, Xue Y, Wang W, Jin F-F (2007) Analysis of ENSO cycle in NCEP coupled forecast model. *J Clim* 20:1265–1284
- Zhang W-J, Li J-P, Jin F-F (2009) Spatial and temporal features of ENSO meridional scales. *Geophys Res Lett* 36:L15605. doi:[10.1029/2009GL038672](https://doi.org/10.1029/2009GL038672)